Single Oxygen Molecule Sensitivity of Organolead Halide Perovskite Photoluminescence

*Juvinch R. Vicente,[1,4] Ali Rafiei Miandashti,[1] Kurt Waldo E. Sy Piecco,[1,4] Joseph R. Pyle,[1] Martin E. Kordesch,[2,3] Jixin Chen[1,3]**

[1]Department of Chemistry and Biochemistry, [2]Department of Physics and Astronomy, [3]Nanoscale and Quantum Phenomena Institute, Ohio University, Athens, OH 45701.

[4]Department of Chemistry, University of the Philippines Visayas, Miagao, Iloilo 5023, Philippines.

ABSTRACT

The photoluminescence (PL) of organolead halide perovskites (OHPs) is sensitive to its surface conditions, especially surface defect states, making the PL of small OHP crystals an effective way to report their surface states. At the ensemble level, when averaging a lot of nanocrystals, the photoexcitation of OHP nanorods under inert nitrogen (N_2) atmosphere leads to PL decline, while subsequent exposure to oxygen (O_2) results to reversible PL recovery. At the single-particle level, individual OHP nanorods photoblinks, whose probability is dependent on both the excitation intensity and the O_2 concentration. Combining the two sets of information, we are able to quantitatively evaluating the interaction between a single surface defect and a single O_2 molecule using a kinetic model. This model provides fundamental insights that could help reconcile the contradicting views on the interactions of molecular O_2 with OHP materials and help design a suitable OHP interface for a variety of applications in photovoltaics and optoelectronics.

Keywords: Nanorod photoblinking, photo-knockout, single-molecule gas absorption and desorption kinetics, super-resolution optical imaging

Organolead halide perovskites (OHP) have emerged as a promising material for applications in photovoltaics and optoelectronic devices.[1–6] More recently, photoblinking has been reported in OHP nanoparticles, i.e., the photoluminescence (PL) from each particle blinks over time during light excitation. It is believed that photoexcited free charge trapping/detrapping on highly-efficient PL quenchers at the surfaces of OHPs is responsible for this phenomenon.[7,8] Thus, PL blinking has been found to be sensitive towards surface adsorbates such as ligands or gases.[9–15]

In particular, it has been shown that exposure of OHPs to molecular O_2 under illumination results to the enhancement of PL, which is believed to deactivate trapping defects within the bulk of the material.[14] On the other hand, detrimental effects of O_2 on OHP PL properties were also reported owing to the adsorption and intercalation of O_2 on OHP surface.[10,11] In both cases, the effects were shown to be reversible to some extent.[16–18] In addition to this reversible effect, exposure of OHPs to O_2 under light irradiation have also been associated with permanent photodegradation, driven by the direct formation and interaction of superoxide species on OHP surfaces.[13,19] The conflicting views on the interaction of O_2 with OHP materials warrant further investigation.

Here we systematically studied the ensemble PL behavior of ligand-protected OHP nanorods over a series of different excitation intensities and O_2 concentrations. To gain mechanistic insights into our ensemble results, we performed a detailed single-particle analysis of the PL behavior of individual OHP nanorods. From our ensemble experiments, we found that the rate of PL decline is positively correlated with the excitation light intensity under very low oxygen concentration but is negatively correlated with the increase of bulk O_2 concentration in the

environment. Moreover, we showed that the PL decline could recover reversibly upon exposure of OHP nanorods to higher oxygen concentration. The reversible PL behavior of OHPs is a consequence of PL intermittency in individual nanorods. These behaviors have been reported in the literature and we adapted a hypothesis from the literature that this phenomenon is facilitated by photocharge trapping and detrapping on the surface defects of OHP nanoparticles.[7–10,20] Specifically, we propose that adsorbed O_2 facilitates passivation of these surface defect states leading to the brightening of nanorods. While passivation mechanism involving O_2 is a reversible pathway to enhance the PL of the nanorods, we confirmed that passivating the surface traps with surface ligands "permanently" suppresses photoblinking and essentially eliminates the PL decline of the OHP nanorods. In the end and new to the literature, we propose a detailed kinetic model to explain all our experimental results, both ensemble and single-particle data in the simplest way to us. To validate our proposed model, we fit all the data globally and performed Monte Carlo simulations and confirmed that our model is consistent with both ensemble and single-particle PL data.

We first synthesized methylammonium lead iodide ($CH_3NH_3PbI_3$) nanorods with an oleylamine/oleic acid ligand-assisted colloidal method[8,21] and confirmed that their optical and morphological properties were consistent with those reported in the literature (**Figure S1**).[8,21] Then, we spread and dried them sparsely on a glass coverslip and made a flow cell to control their gaseous environment (**Figure S1, S4**).

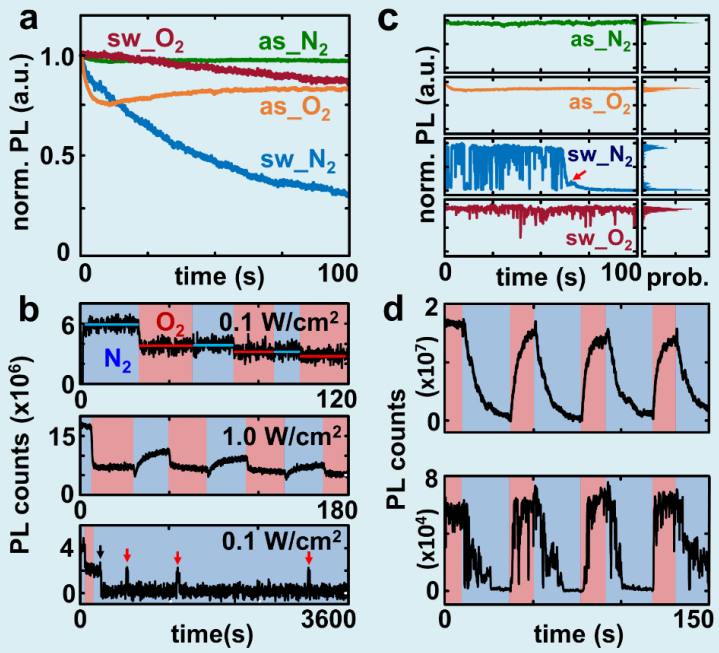

Figure 1. (a) Ensemble PL trajectories of as-synthesized (as) and solvent-washed (sw) nanorods under N_2 and O_2. (b) Ensemble PL of as-nanorods under alternating gas with different laser intensities (top, mid). The black arrow (bottom) indicates when the laser was turned off, and red when it was turned on for ~2 s to check the PL. (c) Representative single-particle PL from (a). (d) Ensemble and representative single-particle PL of sw-nanorods under alternating ambient gas.

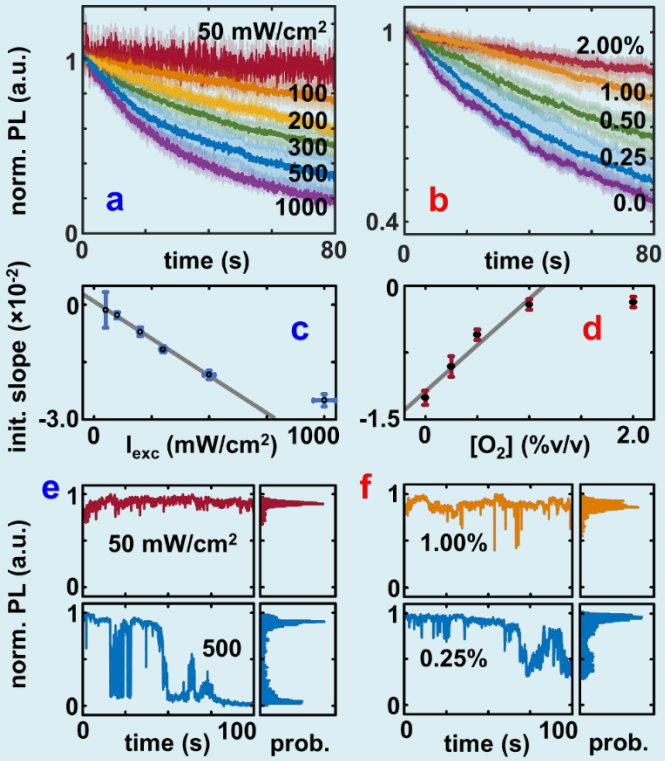

Figure 2. (a) Normalized ensemble PL trajectories of sw-nanorods exposed to pure N_2 under various laser intensities (Movie S2), and (b) O_2 concentrations at constant laser intensity (Movie S3). Each halo in (a, b) represents the error bar, the standard deviation of three measurements. (c) Initial PL-decay rates (first ~10 s) as a function of excitation intensity and (d) O_2 concentrations. (e, f) Representative single-particle PL trajectories in (a) and (b) and their relative probability distributions, respectively. Complete series is shown in **Figure S9-S10**.

In our first measurement, we evaluated the impact of ligand-passivation on the time-dependent PL of the nanorods (**Figure 1**). As-synthesized nanorods (as) are fully protected by ligands[9] when dried, and imperfect ligand protection was obtained by solvent washing (sw) (**S1.1**).[22] The PL of fully ligand-protected nanorods appears stable under both N_2 and O_2, except for an initial decay observed under O_2. We further found out that this initial decay is irreversible under dark or weak illumination, but slightly reversible under stronger illumination. We attribute

this decay to ligand rearrangement under light and O_2. For partially ligand-protected nanorods, the PL declines rapidly upon illumination under pure N_2 but remains relatively more stable under O_2. The PL decline could have been explained by photodegradation of $CH_3NH_3PbI_3$, however, its reversibility under different gases and the consistency of its emission spectrum (**Figure S2**) suggest a different mechanism.

The significant influence of the surface ligands and the ambient gas on the PL of the nanorods strongly suggests the presence of surface trap states. These trap states are likely related to under-coordinated lead ions, methylammonium vacancies, and/or iodide vacancies[8,23,24] that are known to act as effective PL-quenching sites on OHP nanoparticles and thin films.[7–9,25] In the presence of surface ligands, these surface defects are effectively passivated, hence the PL is stable both at the ensemble and at the single-particle level (**Figure 1**), consistent with the recent reports.[9,26,27] On the contrary, OHP nanorods with bare or partial ligand-protected surfaces turn dark under N_2 (**Figure 1c**) due to the activation of the surface defects by photoexcited charge trapping. The activated traps discharge spontaneously and the nanorods turn bright with no expected aid from N_2 and greatly accelerated by the presence of O_2 (**Figure 1c**). The mechanism of PL quenching by a trapped charge has been associated with nonradiative Auger-assisted charge recombination.[28–30] The PL can be quenched by light under N_2 but can recover by sitting in the dark under N_2 (**Figure S7**) or flowing-in O_2 under light (**Figure 1d**, **Movie S1**). The reversibility of this process agrees well with the weak physicochemical interactions of O_2 with OHP.[10,24,31] Since no permanent photobleaching is observed under these conditions, we name the temporary loss of PL under N_2 "*photo-knockout*" (red arrow **Figure 1c**, blue curve) to distinguish it from photobleaching.

The photoexcited charge carriers, which varies linearly with the laser intensity (**Figure S8**), activate the surface traps, and O_2 helps their relaxation (**Figure 2**). We observed that the higher the laser intensity the faster the initial PL decay rate of the nanorods, which has a linear correlation at low laser power densities under N_2 (< 0.5 W/cm^2). This dependence has been observed for larger perovskite microcrystals in the literature.[17] On the contrary, the higher the O_2 concentration, the slower the decay rate, for which a linear relationship is observed at relatively low O_2 concentrations (<1% v/v) (Figure 2d). At relatively high laser intensities and low O_2 concentrations, we observed the stepwise photo-knockout behavior of the single nanorods (**Figure 2e-f**).

Single-nanorod photoblinking analysis (**S2.2**) on the lifetimes of the ON-state (τ_{ON}) and OFF-state (τ_{OFF}) further confirms that the photoexcited charges accelerate charge-trapping and the bulk O_2 molecules facilitate the charge-detrapping (**Figure 3**). Under pure N_2, τ_{ON} is anti-correlated,[30] while τ_{OFF} is not significantly correlated with increasing laser intensity (**Figure 3c-d**). This suggests that photoexcited carriers activate trap states but is not involved in the detrapping process. Under constant laser intensity, τ_{ON} is positively correlated, while τ_{OFF} is anti-correlated with increasing O_2 concentration (**Figure 3f-g**), indicating that the active traps are deactivated and protected by molecular O_2. In addition, single-nanorod super-resolution analysis (**SI S2.3**) shows that the traps are randomly distributed along a nanorod (**Figure 3b**), which are stochastically activated and deactivated over time (**Figure S14−S15**). The change on τ_{ON} and τ_{OFF} over time contributes to the PL decay under O_2 but is insignificant under N_2 (**Figure S13**). Under N_2, the photo-knockout lifetime of the nanorods (τ_{KO}) is responsible for their ensemble PL decay (**Figure 3e**). The saturation of τ_{ON}, τ_{OFF}, and τ_{KO} at 2.0% (v/v) O_2 (**Figure 2d**, **Figure S11**) suggests a diffusion-limited surface adsorption/reaction mechanism.

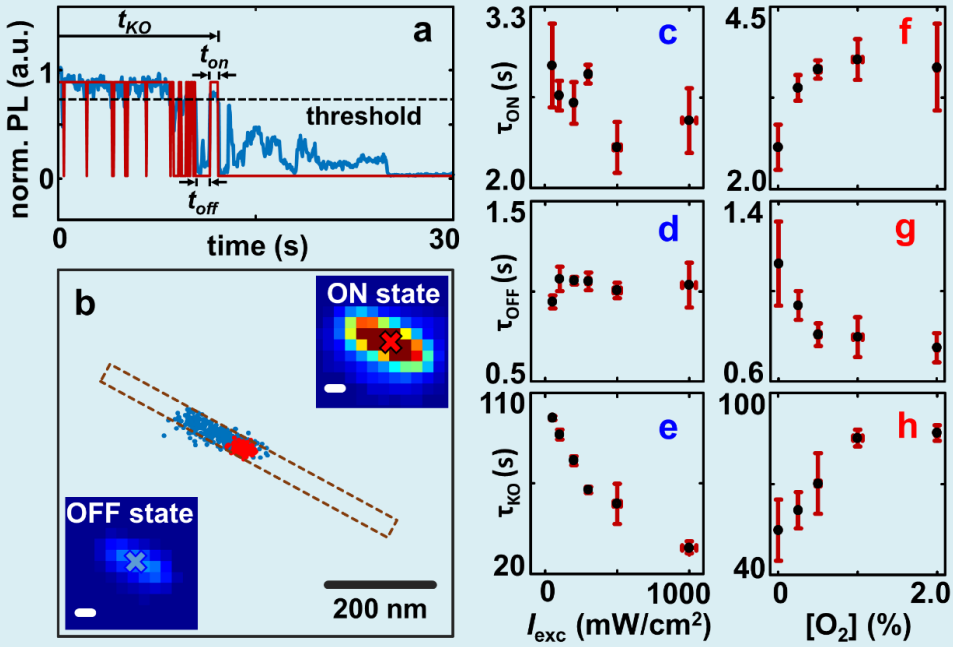

Figure 3. (a) A scheme of photoblinking analysis. (b) Spatial distribution of ON (red) and OFF (blue) states over a single nanorod by super-resolution emission localization. Scale bars = 200 nm. (c-e), The average dwell-times of ON, OFF, and photo-knockout states under different excitation intensities and (f-h) O_2 concentrations in our measuring window (note, they have power-law like distribution thus have no global averages).

Based on observed ensemble and single-particle PL behaviors of OHP nanorods in N_2 and O_2, we propose a kinetic model and fitted the data at a high confidence level ($R^2 \approx 1$, **Figure 4**). In this model, we hypothesize that the quenching of the PL is solely attributed to the activation of an exposed surface defect. To begin with, we assume that the series of solvent washing effectively exposes surface defects that lack ligand-protection, which we label here as, SD, to distinguish them from ligand-protected surface defects, SD^{Lig}. From **Figure 1a**, we know that exposure of OHP

nanorods to O_2 results in PL recovery due to passivation of surface defects with O_2, which we now note as SD^{O2}. Evacuating O_2 and replacing it with N_2 under illumination results to a PL decline (**Figure 1d**). Hence, illumination (*hν*) is capable of kicking off O_2 molecule from the surface defects, which provided the basis for a reversible reaction 1 (**Figure 4a**). The reversible reaction 2 simply illustrates the photoblinking behavior of the nanorods, where SD and SD* represent natural and activated surface defects, respectively. Since the increasing concentration of O_2 results to decreasing average τ_{OFF}, we propose that O_2 facilitates detrapping of a charge from SD* as described in reaction 3 (**Figure 4c**). Finally, when the fully ligand-protected nanorods were exposed in O_2 under illumination, the PL declines, while no decay is observed under N_2 (**Figure 1a**). These experiments suggest that under illumination, O_2 is capable of replacing a surface-ligand even on the fully ligand-protected nanorods while N_2 cannot (**Figure 1c**). The surface ligand, too heavy to escape into the ambient gas, could replace back the O_2 with the aid of light (**Figure 1b**). This process is described in reaction 4 (**Figure 4d**).

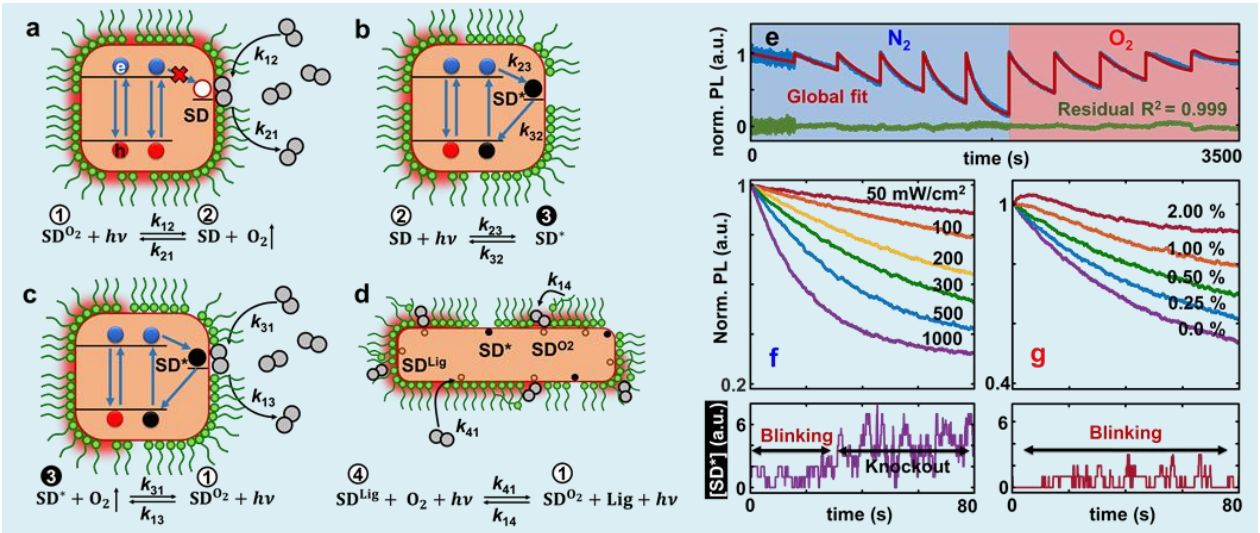

Figure 4. (a-d), Proposed surface reaction mechanism. e, Global fitting of the two sets of data in **Figure 2** using the same parameters from the reaction model. (f,g) Monte Carlo simulated

ensemble accumulated from 5000 individual particles and the representative single-nanorod PL-time trajectories.

The two sets of data in **Figure 2** are globally treated in three steps (**S3**). Briefly, these three steps are (1) analytically fitting the data using approximations to obtain the initial estimates on the parameters shown in **Figure 4a-d**, followed by (2) numerical fitting, and (3) Monte Carlo single-nanorod simulations. The goodness of the numerical fitting and examples of Monte Carlo simulated trajectories are shown in **Figure 4e-g**. The fitting results are shown in **Table S2**. In this model, under pure N_2, all reactions with O_2 as a reactant diminish (i.e. reaction 1, reverse and reaction 3, forward). Thus, both SD and SD* accumulate under illumination over time. Eventually, the SD* concentration will reach a point where at the single-particle level it remains above one per nanorod over time, bringing the nanorod to a photo-knockout state (**Figure 4f**). In the presence of bulk O_2, the O_2-associated reactions in reactions 1 and 4 become significant, which effectively reduces the concentrations of SD and SD*. Thus, photo-knockout is seldom observed when O_2 is present (**Figure 4g**, **Figure S10**) and the average τ_{KO} decreases with the increase in O_2 concentration (**Figure 3h**). This model can also kinetically explain the saturation observed in **Figure 2c** and **2d**, that is, multiple carriers or multiple O_2 molecules at a given time in/on the nanorod create a rate-limiting step.

Interesting information can be obtained from the fitted rate constants (**Table S2**). For example, the rate constant of the light-assisted oxygen desorption $k_d = (k_{12}+k_{13}+k_{14})$ is fitted $4.3\pm0.2\times10^{-2}$ J^{-1} cm^2. Assuming when a small area, A, on the surface absorbs a photon at laser power density P, with 90% probability the oxygen desorbed from the surface. This area A is the effective adsorption cross-section that triggers oxygen desorption. The photon energy of 473 nm

laser is $\varepsilon = 4.2\times10^{-19}$ J, and $k = k_d P = PA/\varepsilon$. Thus, $A = k_d \varepsilon = 1.8\times0^{-20}$ cm^2. This is a very small absorption cross-section, suggesting that only the electron adjacent to or at the adsorbed oxygen, when excited, has the ability to remove the oxygen from the surface while the electrons excited in the bulk has negligible ability to remove the oxygen.

With these results, we hypothesized a mechanism. According to a recent calculation,[11] the energy level of the surface defect lies between the bandgap of the OHP nanorods and connected to the bulk with an energy barrier. When an electron in the bulk is excited, it quickly thermally relaxes to the conduction band edge which still has the ability to go over the energy barrier of a bare surface defect within a time period of seconds and get trapped. But it cannot penetrate the raised energy barrier when an oxygen or a ligand is attached to the surface defect. Only those excited electrons on the defect and carry the extra energy before the thermal relaxation has the ability to penetrate the raised energy barrier.

In summary, we have shown that photoluminescence could be used to probe the surface reactions of OHPs. In particular, we showed that exposure of an OHP nanorod to single O_2 molecules under illumination could result to the enhancement of its PL by facilitating the relaxation of an active trap, and effectively passivating it preventing its further activation. These findings could provide a potential strategy to design a suitable interfacial chemistry for photovoltaic, optoelectronic devices and gas sensors. We further believe that the approach used in this report could be extended to probe other surface phenomena, not only in OHPs but also on other luminescent materials.

Supporting Information

Methods, Data analysis, and Kinetic model

Figures S1 to S16

Tables S1 to S2

ACKNOWLEDGMENTS

We thank Prof. Hugh Richardson for beneficial discussions; Ohio University startup fund; NIH award 1R15HG009972 for supporting the development of data analysis methods.

AUTHOR INFORMATION

Author Contributions

Major experimental design, data analysis, and writing were done by J.C. and J.R.V.; J.R.V collected the major data and the rest of the authors contributed in data collection; all authors read and proved the manuscript.

Competing interests

The authors declare no competing interests.

Corresponding Author

*Jixin Chen: chenj@ohio.edu

REFERENCES

1. Xia, H. R., Li, J., Sun, W. T. & Peng, L. M. Organohalide lead perovskite based

photodetectors with much enhanced performance. *Chem Commun* **50,** 13695–13697 (2014).

2. Hu, F. *et al.* Superior Optical Properties of Perovskite Nanocrystals as Single Photon Emitters. *ACS Nano* **9,** 12410–12416 (2015).
3. Tan, H. *et al.* Efficient and stable solution-processed planar perovskite solar cells via contact passivation. *Science* 722–726 (2017). doi:10.1126/science.aai9081
4. Zhou, H. *et al.* Self-Powered All-Inorganic Perovskite Microcrystal Photodetectors with High Detectivity. *J. Phys. Chem. Lett.* **9,** 2043–2048 (2018).
5. Stranks, S. D. & Snaith, H. J. Metal-halide perovskites for photovoltaic and light-emitting devices. *Nat. Nanotechnol.* **10,** 391–402 (2015).
6. Zhao, X. *et al.* Efficient Planar Perovskite Solar Cells with Improved Fill Factor via Interface Engineering with Graphene. *Nano Lett.* **18,** 2442–2449 (2018).
7. Tian, Y. *et al.* Giant Photoluminescence Blinking of Perovskite Nanocrystals Reveals Single-Trap Control of Luminescence. *Nano Lett.* **15,** 1603–1608 (2015).
8. Yuan, H. *et al.* Photoluminescence Blinking of Single-Crystal Methylammonium Lead Iodide Perovskite Nanorods Induced by Surface Traps. *ACS Omega* **1,** 148–159 (2016).
9. Tachikawa, T., Karimata, I. & Kobori, Y. Surface Charge Trapping in Organolead Halide Perovskites Explored by Single-Particle Photoluminescence Imaging. *J. Phys. Chem. Lett.* **6,** 3195–3201 (2015).
10. Kong, W., Rahimi-Iman, A., Bi, G., Dai, X. & Wu, H. Oxygen Intercalation Induced by Photocatalysis on the Surface of Hybrid Lead Halide Perovskites. *J. Phys. Chem. C* **120,** 7606–7611 (2016).
11. Ma, X. X. & Li, Z. S. The effect of oxygen molecule adsorption on lead iodide perovskite surface by first-principles calculation. *Appl. Surf. Sci.* **428,** 140–147 (2018).

12. Aristidou, N. *et al.* Fast oxygen diffusion and iodide defects mediate oxygen-induced degradation of perovskite solar cells. *Nat. Commun.* **8,** 15218 (2017).

13. Aristidou, N. *et al.* The Role of Oxygen in the Degradation of Methylammonium Lead Trihalide Perovskite Photoactive Layers. *Angew. Chem. Int. Ed. (English)* **54,** 8208–8212 (2015).

14. Tian, Y. *et al.* Mechanistic insights into perovskite photoluminescence enhancement: Light curing with oxygen can boost yield thousandfold. *Phys. Chem. Chem. Phys.* **17,** 24978–24987 (2015).

15. Gheisi, A. R. *et al.* O_2 adsorption dependent photoluminescence emission from metal oxide nanoparticles. *Phys. Chem. Chem. Phys.* **16,** 23922–23929 (2014).

16. Hoke, E. T. *et al.* Reversible photo-induced trap formation in mixed-halide hybrid perovskites for photovoltaics. *Chem. Sci.* **6,** 613–617 (2015).

17. Hong, D. *et al.* Nature of Photoinduced Quenching Traps in Methylammonium Lead Triiodide Perovskite Revealed by Reversible Photoluminescence Decline. *ACS Photonics* **5,** 2034–2043 (2018).

18. Zohar, A. *et al.* Impedance Spectroscopic Indication for Solid State Electrochemical Reaction in (CH3NH3)PbI3Films. *J. Phys. Chem. Lett.* **7,** 191–197 (2016).

19. Aristidou, N. *et al.* Fast oxygen diffusion and iodide defects mediate oxygen-induced degradation of perovskite solar cells. *Nat. Commun.* **8,** 1–10 (2017).

20. Yuan, G. cheng *et al.* The Degradation and Blinking of Single Perovskite Quantum Dots. *J. Phys. Chem. C* acs.jpcc.7b11168 (2017). doi:10.1021/acs.jpcc.7b11168

21. Zhu, F. *et al.* Shape evolution and single particle luminescence of organometal halide perovskite nanocrystals. *ACS Nano* **9,** 2948–2959 (2015).

22. De Roo, J. *et al.* Highly Dynamic Ligand Binding and Light Absorption Coefficient of Cesium Lead Bromide Perovskite Nanocrystals. *ACS Nano* **10,** 2071–2081 (2016).

23. Uratani, H. & Yamashita, K. Charge Carrier Trapping at Surface Defects of Perovskite Solar Cell Absorbers: A First-Principles Study. *J. Phys. Chem. Lett.* **8,** 742–746 (2017).

24. Lu, D. *et al.* Giant light-emission enhancement in lead halide perovskites by surface oxygen passivation. *Nano Lett.* acs.nanolett.8b02887 (2018). doi:10.1021/acs.nanolett.8b02887

25. Merdasa, A. *et al.* "supertrap" at Work: Extremely Efficient Nonradiative Recombination Channels in MAPbI3Perovskites Revealed by Luminescence Super-Resolution Imaging and Spectroscopy. *ACS Nano* **11,** 5391–5404 (2017).

26. Zheng, X. *et al.* Defect passivation in hybrid perovskite solar cells using quaternary ammonium halide anions and cations. *Nat. Energy* **2,** 17102 (2017).

27. deQuilettes, D. W. *et al.* Photoluminescence Lifetimes Exceeding 8 μs and Quantum Yields Exceeding 30% in Hybrid Perovskite Thin Films by Ligand Passivation. *ACS Energy Lett.* **1,** 438–444 (2016).

28. Galland, C. *et al.* Two types of luminescence blinking revealed by spectroelectrochemistry of single quantum dots. *Nature* **479,** 203–207 (2015).

29. Seth, S., Mondal, N., Patra, S. & Samanta, A. Fluorescence Blinking and Photoactivation of All-Inorganic Perovskite Nanocrystals CsPbBr3and CsPbBr2I. *J. Phys. Chem. Lett.* **7,** 266–271 (2016).

30. Wen, X. *et al.* Mobile Charge-Induced Fluorescence Intermittency in Methylammonium Lead Bromide Perovskite. *Nano Lett.* **15,** 4644–4649 (2015).

31. Meggiolaro, D., Mosconi, E. & De Angelis, F. Mechanism of Reversible Trap Passivation by Molecular Oxygen in Lead-Halide Perovskites. *ACS Energy Lett.* **2,** 2794–2798 (2017).

Table of Content: